Duality Derived Transformer Models for Low-Frequency Electromagnetic Transients—Part I: Topological Models

S. Jazebi, *Member, IEEE*, S. E. Zirka, M. Lambert, *Member, IEEE*, A. Rezaei-Zare, *Senior Member, IEEE*, N. Chiesa, Y. Moroz, X. Chen, *Senior Member, IEEE*, M. Martinez-Duro, *Member, IEEE*, T. M. Arturi, *Member, IEEE*, E. P. Dick, *Senior Member, IEEE*, A. Narang, *Senior Member, IEEE*, R. A. Walling, *Fellow, IEEE*, J. Mahseredjian, *Fellow, IEEE*, J. A. Martinez, *Senior Member, IEEE*, and F. de León, *Fellow, IEEE*

***Abstract*—The objective of this two-part paper is to provide clarity to physical concepts used in the field of transformer modeling, to dispel common misconceptions regarding numerical instabilities, and to present unified modeling techniques for low-frequency transients. This paper focuses on proper modeling of nonlinearities (magnetizing branches) since these components are critical to determine the low-frequency behavior. A good low-frequency model should properly represent: normal operation, inrush currents, open and short circuit, out-of-phase synchronization transient of step-up transformers, geomagnetic-induced currents, ferroresonance, and harmonics. This paper discusses the derivation of electrical dual models from the equivalent (magnetic) reluctance networks and the direct application of the principle of duality. It is shown that different dual models need to be derived for different transformer geometries and the advantages and disadvantages of each method are discussed. This paper also compares double-sided versus single-sided dual models, and shows that the double-sided model is a more general approach. The mathematical equivalency of several leakage models (negative inductance, mutual coupling, and BCTRAN) is demonstrated for three-winding transformers. It is also shown that contrary to common belief, a negative inductance is not the source of numerical oscillations, but they occur due to the use of noncorrect topological models for representing the core.**

***Index Terms*—Electromagnetic transients, duality models, low-frequency transients, negative inductance, numerical oscillations, topological models, transformers, transformer modeling.**

Manuscript received July 11, 2015; revised November 12, 2015; accepted January 10, 2016. Date of publication January 25, 2016; date of current version September 21, 2016. Paper no. TPWRD-00914-2015.

S. Jazebi and F. de León are with the Department of Electrical and Computer Engineering, New York University, Brooklyn, NY 11201 USA (e-mail: jazebi@ieee.org; fdeleon@nyu.edu).

S. E. Zirka and Y. Moroz are with the Department of Physics and Technology, Dnepropetrovsk National University, Ukraine 49050 (e-mail: zirka@email.dp.ua).

M. Lambert and J. Mahseredjian are with the Department of Electrical Engineering, École Polytechnique de Montréal, Montréal, QC H3T 1J4 Canada (e-mail: mathieu.lambert@polymtl.ca; jean.mahseredjian@polymtl.ca).

A. Rezaei-Zare and A. Narang are with Hydro One Networks Inc., Toronto, ON M5G 2P5 Canada (e-mail: Afshin.Rezaei-Zare@HydroOne.com; Arun.NARANG@hydroone.com).

N. Chiesa is with Statoil, Trondheim NO-7005, Norway (e-mail: nchie@statoil.com).

X. Chen is with the Department of Electrical Engineering, Seattle University, Seattle, WA 98122 USA (e-mail: xchen@seattleu.edu).

M. Martı´nez-Duró is with Électricité de France R&D, Clamart 92141, France (e-mail: manuel.martinez@edf.fr).

C. M. Arturi is with the Department of Electronics, Information, and Bioengineering, Politecnico di Milano, Milan 20133, Italy (e-mail: cesaremario.arturi@polimi.it).

E. P. Dick is with Kinectrics Inc, Toronto, ON M8Z 5G5 Canada (e-mail: epdick@ieee.org).

R. A. Walling is with Walling Energy Systems Consulting, Clifton Park, NY 12065-1622 USA (e-mail: rwalling@wesconsult.com).

J. A. Martinez is with the Departament d'Enginyeria Elèctrica, Barcelona 08028, Spain (e-mail: jamv@ieee.org).

Color versions of one or more of the figures in this paper are available online at http://ieeexplore.ieee.org.

I. Introduction

TRANSFORMERS are essential components of the power system. Computer modeling and simulation of these devices are complicated because of the interactions of the electric and magnetic fields in a multi-media and non-linear environment (typically iron, oil, paper, and copper). Power transformers behave differently when subjected to the variety of excitations that they face during their lifetime. Accurate transformer models compatible with Electromagnetic Transient Programs (EMTP-type) are of interest for power system modelers. Ideally, a transformer model should be built using the capabilities already available in EMTP-type tools.

The principle of duality is recognized as a physically correct technique to obtain circuital models of power transformers. This technique was first introduced for transformers by Cherry [1] and further developed to include nonlinearities by Slemon [2], [3]. The main advantage of this method is that the physical magnetic circuit of an electromagnetic device can be converted to its dual electric circuit suitable for simulation in EMT-type programs, using standard circuit elements. Duality models are able to describe the distribution of magnetic flux in the core and windings. Therefore, they are capable of providing useful information of the electromagnetic behavior of all transformer construction elements.

There exist other modeling possibilities to represent the physics of magnetic circuits in time domain simulations: bond graphs [4], [5], magnetic circuit equations [6], [7], gyrator-capacitors [8]–[11], and mutators [12]. Some of these techniques are difficult to implement in EMTP-type programs. An implementation of mutators using commonly available coupled R-L

branches has been recently proposed [12], which allows an easy representation of magnetic circuits, offering an alternative to the use of the duality transformation.

A unified and generally accepted model for transformers capable of reproducing their behavior under all low-frequency operating conditions does not exist. There is a gamut of duality-derived transformer models [13]–[30]; each one with some (small or large) variation with respect to the others. This two-part paper attempts to produce a model capable of reproducing all low-frequency transients for transformers. In particular, this unified model should properly represent: normal operation, inrush currents, short-circuit, out-of-phase synchronization, geomagnetic induced currents, ferroresonance, and harmonics. It is demonstrated that dual models for transformers with different winding geometries or core structures are different. However, a unified model can be derived for a given transformer that is capable to reproduce all low-frequency transients. This is demonstrated for a single-phase shell-type transformer in the paper.

The paper discusses two common methods to derive dual models: (1) the traditional method that converts magnetic circuits into electrical circuits, and is called here "reluctance based" after [3]; (2) the method that derives directly electrical circuits from the geometry of the iron core, the so-called "direct application of the principle of duality" [24].

Finally, two leakage models (i.e., negative inductance, mutual coupling) are introduced and applied to the derivation of multi-winding transformer models. They are also compared to BCTRAN model [31]. The differences between the three approaches are highlighted using a numerical example based on terminal measurements of a four-winding transformer.

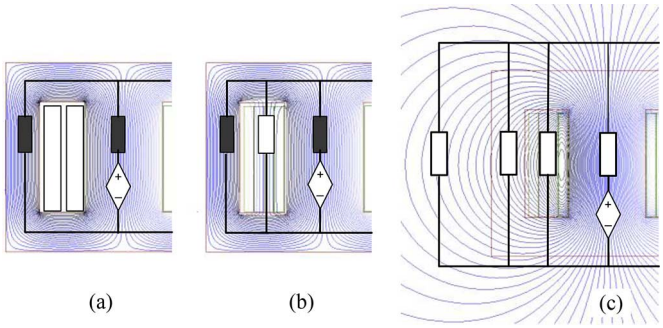

Fig. 1. Magnetic flux density simulated in finite elements for different operating conditions. The reluctance network is shown on top of the transformer window: (a) open circuit; (b) normal operation; (c) high saturation. The black and white rectangles represent nonlinear and linear reluctances, respectively.

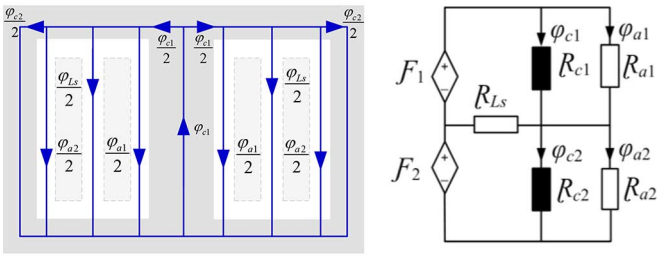

Fig. 2. (a) Flux paths in a shell-type single-phase transformer; (b) equivalent magnetic circuit, after simplifications. The black and white rectangles represent the nonlinear and linear reluctances, respectively.

II. Duality-Based Transformer Models

This section is dedicated to compare two common methods to obtain the topology of dual transformer models.

A. Models Derived From the Magnetic Circuit

The conventional method to derive dual transformer models is based on the conversion of the reluctance network into an electrical circuit [3]. Reluctance networks are built from the connection of reluctances corresponding to the path of magnetic flux in the transformer. Field lines in different transformer designs (*e.g.* shell-type, core-type, welding, and toroidal) are different. Hence, topological models for various geometries are different. A variety of models may result from different geometries of the core, number of windings, construction of windings, number of phases, or construction of tank and accessories. Moreover, a particular transformer has different electromagnetic behavior under different operating conditions such as open circuit, deep saturation, under load, or short circuit. Three different flux patterns are shown in Fig. 1 for open circuit, normal operation, and high saturation. In Fig. 1 the corresponding reluctance circuits for this shell-type transformer are also shown. According to this figure, one may use different topological models for different studies for the same transformer. However, power system modelers need a unified model that is general to use at least for a given geometry under different operating conditions. They can build a comprehensive model with all possible flux paths if the geometrical data is provided. However, manufacturers, rarely (if ever) give internal information about large transformers. Frequently, however, to obtain a very detailed model (reluctance network for all possible flux paths), the complete internal information is needed. Therefore, in this paper optimum models with the minimum number of components useful for all low-frequency transients are recommended. For instance, for a shell-type transformer, this can be appreciated by representing the flux paths of Fig. 2(a). Converting these flux paths into an equivalent magnetic circuit gives the model shown in Fig. 2(b) (exploiting symmetry to simplify the circuit). The magnetomotive force (mmf) sources are inserted into the magnetic circuit so that loops surrounding windings integrate the corresponding mmf, as explained in [32]. Then the electrical equivalent circuit is derived from the principle of duality, where reluctances become inductances, nodes become loops and loops become nodes, and mmf sources (current-controlled voltage sources) become current-controlled current sources. Conventionally, the dual electrical models derived from the magnetic circuits are equipped with ideal transformers as shown in Fig. 3 [2]. The winding resistances are added to the external terminals of the ideal transformers. Also, a capacitance network may be connected at the external terminals, if necessary, to take into account the capacitances to ground and the inter-winding capacitances.

The hysteretic inductors can be represented with static or dynamic hysteresis models to represent the core losses. Also, they can be substituted with non-hysteretic inductors (piecewise

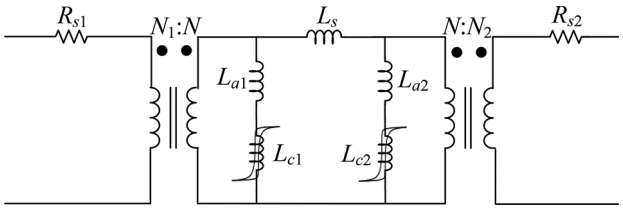

Fig. 3. Duality derived π model.

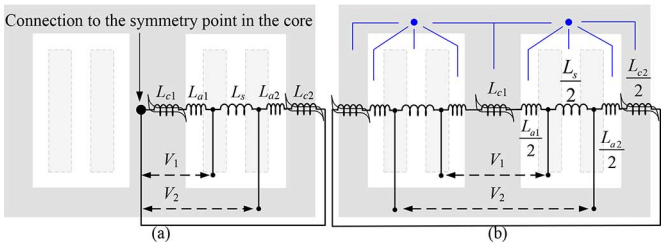

Fig. 4. Derivation of the dual circuit for a shell-type two-winding transformer using direct application of the principle of duality: a) Conventional single-sided derivation; b) Double-sided derivation; the flux paths used for the direct derivation of the circuit are shown.

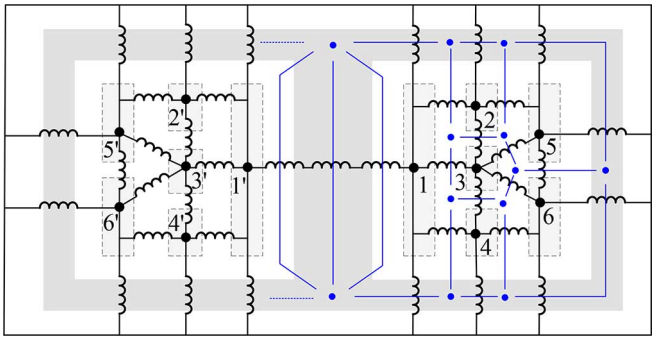

Fig. 5. Direct application of the principle of duality on a shell-type transformer with a special winding configuration; the flux paths used for the direct derivation of the circuit are shown.

linear approximation) for transient studies where the core losses are insignificant (see Part II).

The use of ideal transformers is strongly recommended for duality derived models. There are two important reasons to use ideal transformers in topology derived models: accuracy and physical consistency. When calculating the inductors of the dual circuit, they are referred to a common number of turns (commonly $N = 1$). Hence, to achieve the correct terminal behavior, ideal transformers (with turns ratio $N : N_i$) are required to reflect the correct equivalent inductance from all terminals while maintaining the proper voltage conversion between windings. Frequently the solutions of the dual models with/without ideal transformers match. However, there are cases for which the presence of ideal transformers is indispensable: the external connection (i.e., Y, Δ, or Zigzag) of terminals in three-phase transformers and mid-frequency models including eddy current and capacitive effects. Short circuits of some of the inductors are experienced when ideal transformers are not used for three-phase transformers in the presence of Δ connections. In fact, the solutions obtained from circuits with/without ideal transformers are different for three-phase transformers. Also, these ideal transformers facilitate the series and parallel connections of different windings and/or winding sections, required for some mid-frequency dual models, while providing appropriate terminals to connect the capacitances [29].

Note that, the inductors obtained from the principle of duality represent the magnetic behavior of the device (i.e., they model the circulation of magnetic flux), while resistors represent losses and capacitors deal directly with electric charges, which are completely different in nature. The ideal transformers isolate the electrical parts from the magnetic parts.

B. Direct Application of the Principle of Duality

The dual electrical equivalent can be obtained directly from the geometry of the transformer without drawing the reluctance circuit. In many occasions (for general multi-winding transformers or multi-sections for high-frequency) it can difficult to identify the connection points of the terminals from the reluctance circuit. These connection points are very clear when assembling the model directly from the geometry (as simple as connecting the terminals at the location of the windings or sections) [24]–[29]. For a symmetrical geometry such as a shell-type transformer, the direct application of principle of duality could be implemented on half part of the geometry (single-sided) or both parts of the geometry (double-sided) [29]. To illustrate this, consider the model for shell-type two-winding transformers shown in Fig. 4. For the single-sided approach (of Fig. 4(a)), the winding connections are made to the symmetry point at the center of the core, while the double-sided procedure (of Fig. 4(b)) reveals the primary and secondary terminals effectively. Since the geometry is completely symmetrical, the circuit derived from Fig. 4(b) is perfectly equivalent to the one of Fig. 3, since the symmetrical inductances are virtually in series (currents are the same). However, some care is usually needed to identify the correct terminal connection points for a single-sided transformer model.

For geometries including more windings (or winding sections), as shown in Fig. 5, it is less intuitive to insert the connection points when using the reluctance-based method. One needs to propagate the mmf source in the central limb, as explained in [32]. However, as shown in Fig. 5, the electrical dual model can be directly drawn on top of the transformer window by the direct application of the principle of duality. The terminal connections are clearly identified on the corresponding windings. The ideal transformers are then added to the electrical circuit in Fig. 6. The winding resistances are not included because of lack of space. The capacitors could be connected after the ideal transformers if required. The significance of the terminal capacitances is highlighted in Part II of this paper.

Transformer modelers can skip the step of deriving the magnetic circuit and directly derive the electric equivalent circuit on top of the geometry drawing (assuming flux paths), so that the direct application of the principle of duality is a shortcut that allows faster derivation of topological models. However, the resulting model will be the same as with classical duality, as seen when comparing Figs. 3 and 4(a).

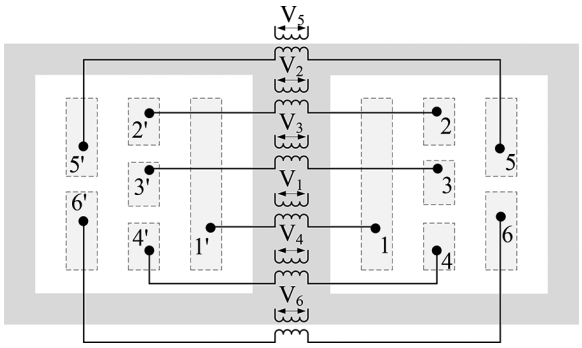

Fig. 6. Connection of the ideal transformers to the model of Fig. 5.

Double-sided dual models are necessary for some mid-frequency models that take into account the eddy current and capacitive effects [29]. In this condition, the electrical connections for ideal transformers cannot be identified with single-sided reluctance-based models. Also, in single-sided models there are not sufficient terminals to connect the capacitors that represent the insulation layers.

III. Numerical Stability of Multi-Winding Transformer Models

In this section, the most popular leakage inductance models for multi-winding transformers are reviewed and compared.

A. Introduction to Terminal Leakage Models

There are three different approaches for representing leakage in topologically-based core models for multi-winding transformers; they are based on the use of: (1) Negative Inductances (NI); (2) Mutual Couplings (MC); and (3) BCTRAN.

The so-called *Negative Inductance* (star equivalent) model was first introduced by Boyajian in 1924 [33]. The model was designed for steady state behavior. The magnetizing branches are neglected in the first Boyajian's publications [33], [34]. Later, the model was expanded to include the nonlinearities of the iron core in the equivalent circuit [35]. According to the theory of the three-circuit transformers [35], a three-winding transformer can be represented with a four-terminal network in which all terminals are connected to each other with an inductor. Reference [35] calls the model shown in Fig. 7(a) "exact" or "ideal".

The non-linear inductors connected to node 0 represent the excitation characteristic of the transformer. The magnetizing currents are very small under *steady state* conditions. Therefore the model shown in Fig. 7(a) can be simplified to the model shown in Fig. 7(b). This model is converted to equivalent circuit of Fig. 7(c) with Δ-Y transformation. Because of the complex procedure required to determine the non-linear parameters of the "exact" model, a single magnetizing branch was added to the middle node as a bulk component [35]. The ideal transformers and terminal resistances are then added to obtain the model shown in Fig. 8. Hence, the location of the magnetizing branch in Fig. 8 was decided for convenience and it is not physically sound.

The (wrong) location of the magnetizing branch may also be inherited from the traditional T (Steinmetz) model for a two-winding transformer (see Fig. 9). This classic model has been used successfully for over 100 years for steady state analysis, but since it is not a topologically correct model, it frequently fails to properly represent the behavior of a transformer under saturation [23], [27]. Despite the lack of physical meaning, the Steinmetz equivalent is still acceptable for rated steady-state conditions when the magnetizing branch can be neglected (low saturation). The unrealistic nature of the T-model becomes evident when the core approaches saturation, for example, during inrush current events. Nevertheless, for a standard three-winding transformer design, the value of L_2 is negative [24], [36], the reason why the model is called *negative inductance model* in this paper.

A subject of debate over the past three decades [24], [30], [36]–[38] has been the numerical instability apparently caused by the negative inductance (L_2) in the star-equivalent circuit of a three-winding transformer as shown in Fig. 8. The instability has been mathematically proven in [36] and [37], but the

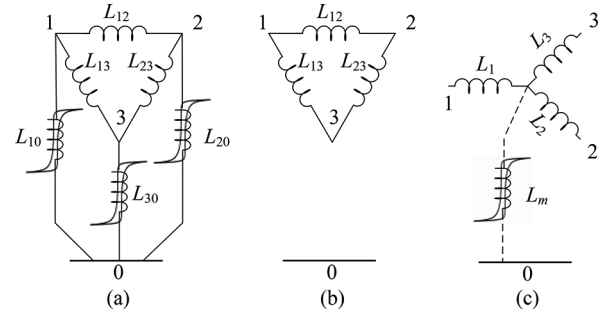

Fig. 7. Equivalent circuits for three-winding transformers [35]; (a) exact representation; (b) delta representation when excitation current is neglected; (c) equivalent star representation when excitation branch is added to the center point. Note that, the connection of the inductor L_m is arbitrary and not justified on a rational basis: the star center is a mathematical node emerging from the delta-star transformation, which cannot be used to connect any magnetizing inductor or a resistor to represent the core losses.

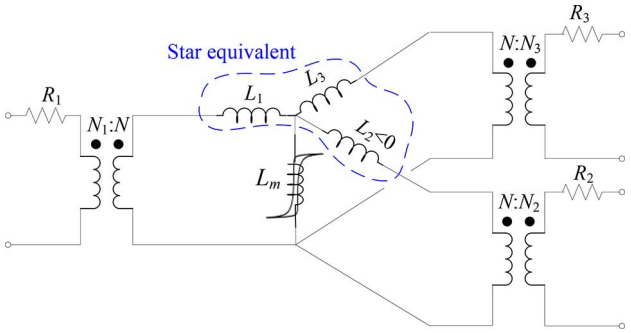

Fig. 8. Star representation of a three-winding transformer. Inductance L_2 associated with the middle winding is negative.

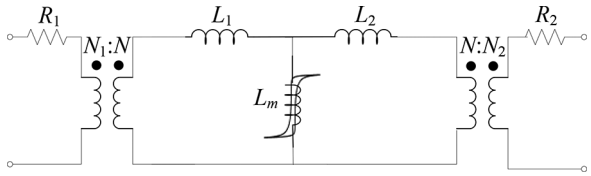

Fig. 9. Traditional representation of a two-winding transformer (T-model). There is substantial experimental evidence showing that this model fails to properly represent the transformer under heavy saturation.

real problem was not revealed. The true reason of the numerical instability is not the use of the negative inductance L_2, but not considering the transformer topology, which has resulted in the erroneous location of the magnetizing branch at the center of the star. Conventionally, a resistor represents the core losses in parallel with a lossless inductor [39]. However, as discussed earlier, in this paper, the hysteresis inductors represent the core losses. In the literature, one can find solutions proposed to prevent oscillations of the circuit of Fig. 8, such as: connecting the magnetizing resistance to one of the terminals or distribute them among all terminals [36], autotransformer-based solutions [37], and relocation of magnetizing branch to the inner winding terminal based on the principle of duality for a core-type transformer which has no iron outside the outer windings (for all phases) [30]. Note that, core-type units are more common than shell-type units at high power ratings.

The other alternative is to completely avoid negative inductance values using a mutual coupling model. This model was first introduced for three-winding transformers in [24] and later extended to multi-winding cases in [26]. It is noteworthy to mention that mutual inductances have been used to model the effects between different phases in [16].

Note that [24], as some other publications [36], wrongly blames the numerical instabilities to the negative inductance. In fact, the negative and the mutual coupling inductance models are mathematically equivalent for a three-winding transformer. The following section shows that when the magnetizing branch is located correctly there are no numerical instabilities.

B. Physical Interpretation of the Negative Inductance

Negative inductors are frequently used to model the leakage inductances of multi-winding transformers. The first physical interpretation of the negative inductance was introduced by Boyajian [33]. However, in this paper, a more scientific approach is introduced to shed light into its physical meaning. The 2D arrangement shown in Fig. 10(a) consists of two concentric windings 1 and 2 that are separated by a distance d_{12}. Assuming there is no fringing flux (all windings have the same height and are close to the yokes), the "total" leakage inductance L_{12} is calculated using the well-known expression [3], [24]:

$$L_{12} = \frac{\mu_0 N^2 l}{l_c} W_{12}. \tag{1}$$

where l is the mean length of the turn; l_c is the mean length of the magnetic flux path; W_{12} is the *effective* width of the leakage channel. W_{12} is traditionally determined from the trapezoidal distribution of the magnetic field strength (H) in the transformer window used by many researchers [24], [30]. The expression for the leakage channel is given as function of the winding thicknesses a_1, a_2, and the separation distance between them d_{12} as follows [3]:

$$W_{12} = \frac{a_1}{3} + d_{12} + \frac{a_2}{3}. \tag{2}$$

Equations (1) and (2) are used for the calculation of leakage inductance between two windings with the same current in opposite direction. The distribution of the magnetic field is assumed to follow a trapezoidal pattern [3]. For three-winding

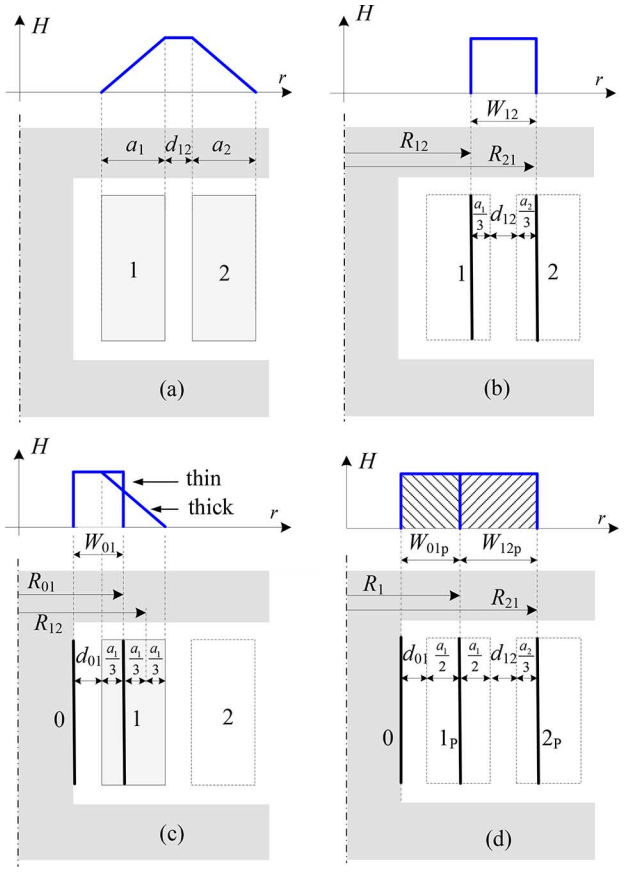

Fig. 10. Representation of the transformer window (shell-type two-winding) including the distribution of the magnetic field in short circuit conditions: (a) thick winding representation; (b) thin winding representation; (c) equivalent between core (winding "0") and winding 1 (thick and thin) for the flux linking the core; (d) equivalent between core winding "0" and windings 1_p and 2_p.

transformers, the magnetic flux pattern/amplitude change when a different pair of windings is energized. The magnetic flux in the region between the two conductors (air) is completely uniform as shown in Fig. 10(a). Hence, the flux pattern of this part does not change for the short circuit tests between any pair of windings. However, a difference exists for the magnetic flux that passes through the thickness of the conductors (linear decaying or rising pattern). As discussed in [24], this portion of the magnetic field causes a mismatch for one of the short circuit tests in a three-winding transformer. As an alternative, the total magnetic flux can be reconstructed with a uniform magnetic flux distribution that is produced by *zero thickness windings*. For simplicity, the approach is described in this paper with a two-winding transformer. However, the same concept can be extended for three-winding transformers.

For a two winding transformer, the leakage channel W_{12} can be seen as separating two infinitely thin windings with radii R_{12} and R_{21}; see Fig. 10(b). Also, a fictitious winding with zero thickness is considered on the core. To explain the nature of the negative inductance, consider the flux distribution between a fictitious winding located at the core (winding "0") and winding 1; see Fig. 10(c). Short circuit between two thin windings "0" and "1" emulates the flux linking the core. The *effective* width

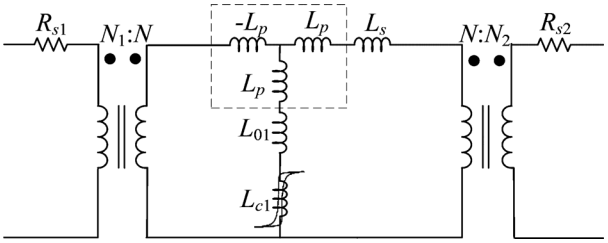

Fig. 11. Two-winding shell-type transformer model with negative inductance.

W_{01} of the channel between the core and the real (thick) winding 1 is:

$$W_{01} = d_{01} + \frac{a_1}{3} \tag{3}$$

where d_{01} is the space between winding 1 and the imaginary thin winding 0 situated on the core surface [21]. Winding 1 can be represented by a thin winding of radius $R_{01} = R_{12} - a_1/3$. Comparing Fig. 10(b) and (c), winding 1 can be characterized by two thin windings with different equivalent radii, R_{01} and R_{12}. To resolve the ambiguity and construct a unique model, winding 1 can be represented by a *thin* winding $1_{\rm p}$, with radius R_1 equal to the mean radius of the real winding; see Fig. 10(d). Also, winding 2 can be represented by a thin winding $2_{\rm p}$ with radius equal to R_{21}. Hence, the model of Fig. 10(d) can be obtained with three thin windings (0, $1_{\rm p}$, and $2_{\rm p}$). The next step is to compute the parameters of Fig. 10(d) according to the geometrical information, so that the leakage inductances computed from Fig. 10(a) and (d) match. For this reason, inter-winding distances should be equal to $W_{01{\rm p}} = W_{01} + a_1/6$ and $W_{12{\rm p}} = W_{12} + a_1/6$. By analogy with (1), the terms $a_1/6$ in these formulae can be represented by the following inductance [30]:

$$L_{\rm p} = \frac{\mu_0 N^2 l}{l_{\rm c}} \frac{a_1}{6}. \tag{4}$$

The leakage inductance between windings $1_{\rm p}$ and $2_{\rm p}$ is given by: $L_{12{\rm p}} = L_{12} + L_{\rm p}$. Similarly, the leakage inductance between windings "0" and $1_{\rm p}$ is $L_{01{\rm p}} = L_{01} + L_{\rm p}$. Thus the leakage model should include a negative inductance $(-L_{\rm p})$ in series so that the leakage inductance for the thin equivalent windings matches the behavior of the actual thick windings. Using the principle of duality, the leakage model should be supplemented with the core (connected to the fictitious winding "0"), ideal transformers, and winding resistances; see Fig. 11.

This Γ-model arises from the fact that the return path (side leg of the core) has not been modeled; when completed it would become similar to π-model of Fig. 3. The π-model of Fig. 3 is recommended to represent these transformers [23], [27]. The circuit of Fig. 11 has the same leakage inductance between the two windings, comparing to Fig. 3, when neglecting the currents in the magnetizing branches. In this circuit, the magnetizing branch $(L_{01} + L_{\rm c1})$ is connected to the *inner* winding terminals. The same *inner* connection of the magnetizing branch was recommended in [30], [31]. Note that the negative inductance (L_p) is required to accurately take into account the winding thickness.

It is worth remarking that by parameter tuning the model of Fig. 11 can become reversible. A reversible model can be used to compute low-frequency transients involving high saturation (inrush, GIC, etc.), from all terminals, without modification of the circuit parameters [23], [27]. This is because a reversible model is able to reproduce simultaneously the "terminal" saturation inductances L_{1SAT} and L_{2SAT} measured from primary and secondary terminals. Under saturation $(L_{c1} = L_{m\_sat})$ [23], [27], [28], where L_{m_sat} is the component saturation inductance of the branch L_{c1}. Therefore, the following equation can be written:

$$L_{1SAT} = L_{01} + L_{m\_sat}. \tag{5}$$

Also, looking from the secondary side under saturation conditions:

$$L_{2SAT} = L_s + 2\,L_p + L_{01} + L_{m\_sat}. \tag{6}$$

Note that, L_p can be calculated from (4). Also, the values of L_{1SAT} and L_{2SAT} can be obtained from terminal measurements or finite element calculations [42]. Hence, L_{01} and L_{m_sat} can be computed by solving the system of two equations with two unknowns given by (5) and (6).

According to the explanation above, the model of a three-winding shell-type transformer can be derived with the direct application of the principle of duality (see Fig. 12). In this figure, L_{12} and L_{23} are the leakage inductances measured (or calculated) for windings 1–2 and 2–3 respectively. Since the leakage inductance L_{13} measured between windings 1 and 3 for standard transformer designs, especially large power transformers, is usually greater than $L_{12} + L_{23}$, then two positive inductances,

$$L_{p2} = [L_{13} - (L_{12} + L_{23})]/2, \tag{7}$$

and one negative inductance, $-L_{\rm p2}$, are included in the model to match the measured values of L_{12}, L_{23}, and L_{13} simultaneously. The model is further developed to the one presented in Fig. 13, incorporating the terminal resistances and ideal transformers. Remark that the *leakage* part of the model in Figs. 12 and 13 coincides with that in the model of Fig. 8. The negative inductance equivalent can also be substituted with the mutual couplings as shown in Fig. 12. This is because the mutual couplings and the negative inductance models are mathematically equivalent for a three-winding transformer [24]. In this case, the equivalent circuit of Fig. 14 can be derived.

It should be noted that, in transformer models, the number of the core sections (hysteresis inductors) is independent from the number of windings and can be different. For example, in Fig. 12, the iron core is divided in three sections that are represented with three magnetizing branches. However, some authors use one or two sections to represent the low-frequency behavior of the transformer core (frequently because of lack of the design data). Accordingly, magnetizing branches L_{m2} and L_{m3} of Fig. 13 is often lumped into L_{m1}. In this case, numerical instabilities do not happen since the location of the magnetizing branch is correctly identified at the inner winding terminal [30]. However, it is not always possible to have a mathematically correct model behavior from all terminals with only one magnetizing branch. Ideally, transformer models require n sections for an n-winding transformer to accurately represent the behavior seen from all terminals [28].

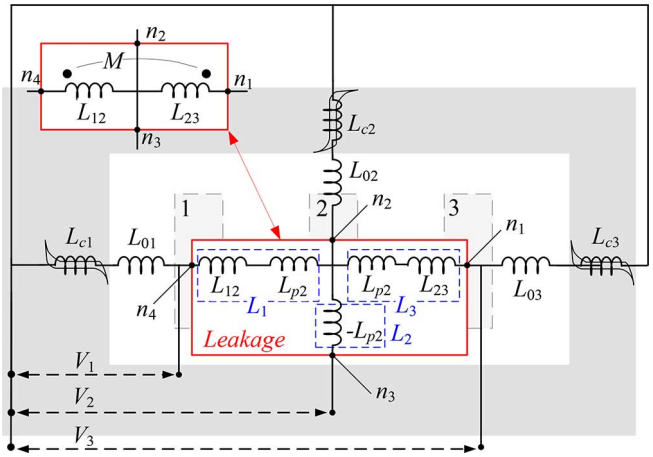

Fig. 12. Direct application of the principle of duality for a three-winding shell-type transformer. Note that, the leakage part can be either represented with negative inductances or mutual coupling models.

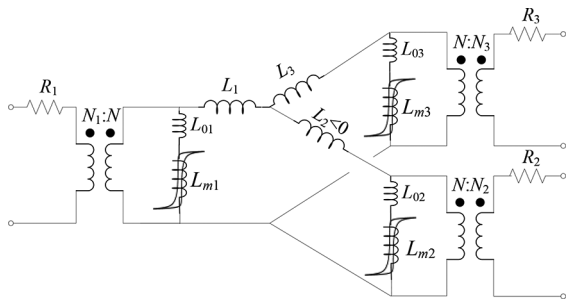

Fig. 13. Three-winding transformer model with three magnetizing branches derived with the application of the principle of duality.

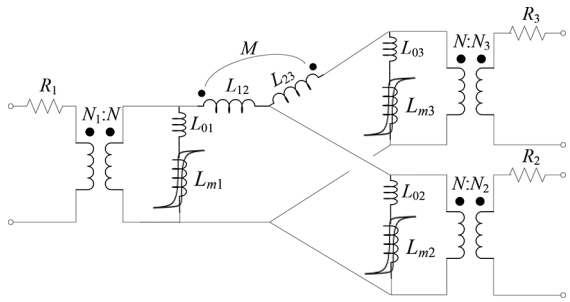

Fig. 14. Three-winding transformer model with three magnetizing branches and mutual coupling leakage model.

There are always "air" flux paths in parallel to iron sections of the magnetic circuit (between windings and the core) that need to be included as series inductances in a dual model. These are L_{01}, L_{02}, and L_{03} in Fig. 12. Their role is to represent the fringing magnetic fluxes, which flow roughly parallel to the iron branches. These components avoid the non-physical situation of having a very high flux in the iron and zero flux in the space around the yoke (air/oil) [40]. In high saturation, the incremental permeability of the magnetic material is the same as the surrounding media (μ_0). Therefore, magnetic flux flows in both the iron core and the surrounding media. In other words, these inductances are needed to reproduce the dispersion of the magnetic flux paths beyond the core when the core sections approach saturation. Thus, these elements are significant under saturation condition, and consequently important to predict the low-frequency transients involving deep saturation.

C. Comparison of the Models' Behavior

In this section, the leakage models (Negative Inductance (NI), Mutual Coupling (MC), and BCTRAN) are compared versus measurements in steady state conditions. Additionally, the numerical stability of three-winding transformer models is investigated.

1) Terminal Behavior Under Steady State Conditions: It has been mathematically proven that the MC and the NI models are equivalent for three-winding transformers to represent the leakage inductance [24]. However, for an n-winding transformer, the negative inductance model gives $2n-3$ degrees of freedom. This is always less than the $n(n-1)/2$ possible short circuit measurement combinations for $n > 3$. Hence, the set of equations to calculate model parameters are always over-determined for $n > 3$. For example, for a four-winding transformer the short circuit measurement between one pair of windings (1 out of 6 combinations) cannot be mathematically reproduced. Similarly, for an n-winding transformer $n(n-5)/2+3$ combinations cannot be exactly represented. However, experiments show that for the tested 4-winding 1 kVA transformer, with geometrical information presented in [27], NI model is accurate enough (see Fig. 15(a)). This model reproduces all the measured leakage inductances except L_{S14}. The inaccuracy in predicting L_{14} is not expected to be significant when model parameters are computed correctly for concentric windings of the same height. The leakage inductances measured and those reproduced by MC and NI models for this 4-winding transformer are presented in Table I. The results are also compared to the well-known and accurate BCTRAN model for the representation of the leakage inductance. Larger inaccuracies may be expected for transformers with more windings or when the winding heights are different. There is still a debate among the researchers (even the authors of this paper) on the scopes and limitations of the negative inductance model and its applicability beyond three windings.

The value of $L_{p2} = 30.35\ \mu$H in Fig. 15 is calculated with (7). A similar formula yields $L_{p3} = 23.7\ \mu$H. Thus, the total inductance $L_{14} = L_{12}+2L_{p2}+L_{23}+2L_{p3}+L_{34} = 1076.7\ \mu$H; this is only 2% less than the measured $L_{14} = 1100\ \mu$H. As one can see from Table I, the mutual coupling model can be used to reproduce the exact leakage inductances [26]. This method also allows one to reproduce the leakage model for any winding configuration. The mutual coupling method has been validated experimentally in [41] for transformers of 96 and 360 MVA. Note that the results on Table I are identical to the BCTRAN model [31] for all models (except L_{14} for the NI model) demonstrating their mathematical equivalence.

2) Numerical Stability: Several models are investigated for a shell-type three-winding transformer using the benchmark example of [36]. The first model is the unstable circuit of Fig. 8 with parameters presented in Table II (benchmark). It is worth mentioning that in this case the magnetizing inductance L_m is considered linear and lossless according to [36]. The core losses are considered with a constant resistance R_m in

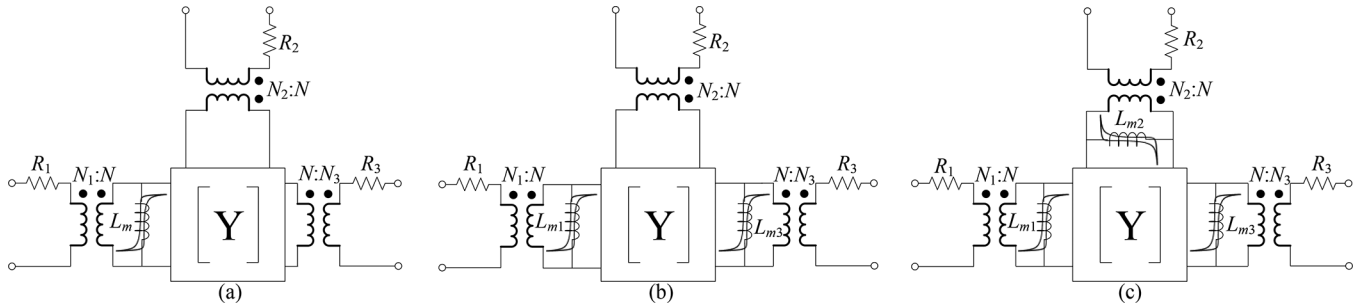

Fig. 15. BCTRAN-based model for three-winding transformer: (a) with only one magnetizing branch on the inner winding; (b) with two magnetizing branches, one on the innermost winding and another one on outermost winding (Hybrid Model); (c) with three magnetizing branches connected to the three windings.

TABLE I
LEAKAGE INDUCTANCES OF A 4-WINDING 1 KVA TRANSFORMER MEASURED, AND REPRODUCED BY MUTUAL COUPLING (MC), NEGATIVE INDUCTANCE (NI), AND BCTRAN MODELS [μH]

	L_{12}	L_{13}	L_{23}	L_{24}	L_{34}	L_{14}
Measured	288	687.8	339.1	728	341.5	1100
BCTRAN	288	687.8	339.1	728	341.5	1100
MC	288	687.8	339.1	728	341.5	1100
NI	288	687.8	339.1	728	341.5	1076.7

parallel with L_m. This example is not a transient case, but a normal open circuit test.

The second model is presented in Fig. 13. The leakage inductances and terminal resistances are as per Table II. Note that, similar hysteresis loops are measured from the different windings of a multi-winding transformer when excited with *nominal voltage*. This is so because at rated voltage the magnetic flux is concentrated in the iron core that passes through an almost similar magnetic path when seen from all terminals. Therefore, as discussed before, the magnetizing branches could be distributed either equally between terminals or lumped on the inner-most terminal. Here, the magnetizing inductance is equally distributed to the terminals ($L_{m1} = L_{m2} = L_{m3} = 1.011$ H and $R_{m1} = R_{m2} = R_{m3} = 762\ \Omega$). Note, however, that in practice, the magnetizing branches should be distributed using the geometrical information of the core and windings, or terminal measurements (see for example [24] and [28]).

The third model is the equivalent three-winding circuit with mutual couplings depicted in Fig. 14. For this case, $L_{12} = 133.2\ \mu$H, $M = 34.3\ \mu$H, $L_{23} = 1.4132$ mH. Note that, to be consistent with the model of Fig. 8, parameters $L_{01} = L_{02} = L_{03} = 0$ in this study (see Figs. 13 and 14).

The last cases correspond to different BCTRAN models. In this section, the BCTRAN model is complemented with magnetizing branches in Fig. 16. The nonlinearities of the core can be distributed either equally between terminals or lumped on one of the terminals. All possible combinations are presented in Fig. 16, including the well-known Hybrid Model [20].

For all models, the transformer is energized from the second winding $V_2 = 199.2$ kV [36]. The voltage of the primary terminal (LV) is shown in Fig. 17. One can observe that the correct connection of the magnetizing branches (Fig. 13) gives stable simulations while the model shown in Fig. 8 shows numerical instabilities. All BCTRAN-based models of Fig. 16 show stable responses.

TABLE II
PARAMETERS FOR THE MODEL OF FIG. 8

R_1 [mΩ]	R_2 [mΩ]	R_3 [mΩ]	L_1 [μH]	L_2 [μH]	L_3 [mH]	R_m [Ω]	L_m [mH]
1.25	0.26	2.6	185	-16.84	1.43	254	337

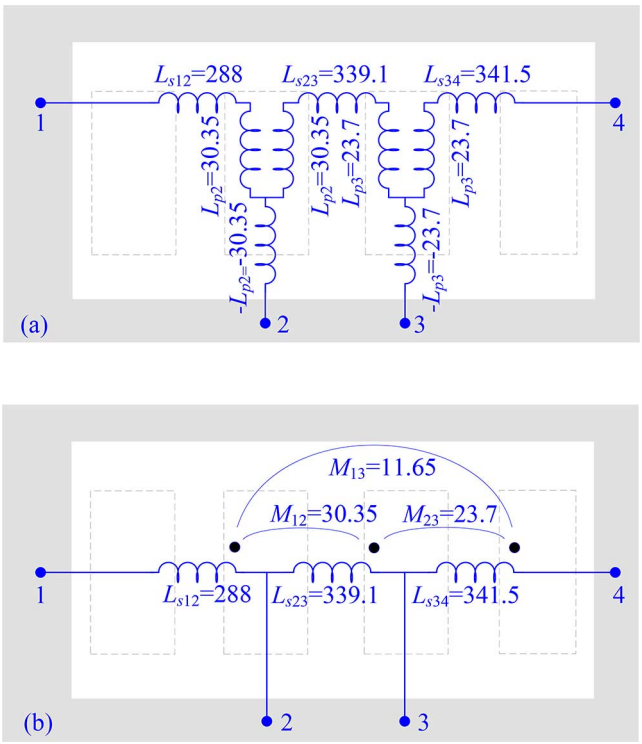

Fig. 16. Leakage inductance models for the four-winding transformer with concentric geometry of the coil: (a) negative inductance model with $L_{p2} = M_{12}$ and $L_{p3} = M_{23}$; (b) mutual coupling model.

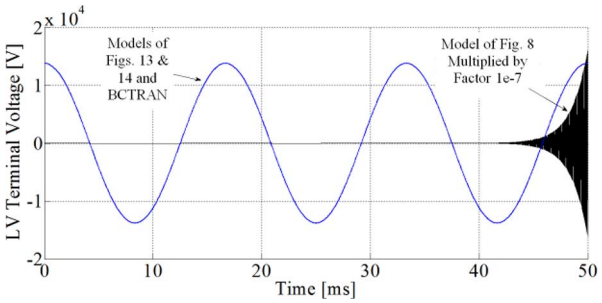

Fig. 17. Performance comparison of the models of Figs. 8, 13, and 14.

3) Discussion: BCTRAN gives a perfect representation of the leakage inductance seen at terminals. However, it cannot represent the core in a dual sense since it is obtained from terminal measurements in short-circuit. Indeed, the core needs to be connected to BCTRAN in an artificial manner.

There have been some attempts to connect the BCTRAN leakage model to duality-derived models for the iron core; these are the so-called hybrid models [20]. These models provide physical connection points between the dual core model and the terminal leakage model. However, not all physical connection points between the core and windings are available. The connections are made at two points, one at a fictitious winding located at limb and the other is given by the external winding.

For three-winding transformers all (leakage) models discussed in this paper are equivalent. However, the connections of the leakage models to the core models are different. The negative inductance and the mutual coupling models can be connected to the core model in a completely dual manner. BCTRAN lacks the proper number of connection points to the core. Connections of the dual core model to the BCTRAN leakage model are made through fictitious windings. Therefore, the resulting transformer model is not completely dual since the core is not "dually connected" to the windings. The negative inductance and mutual coupling models eliminate the need of using fictitious windings to create a topological correct model including core and windings.

In conclusion, the performance of the negative inductance and mutual coupling models would not be theoretically identical to BCTRAN and hybrid models. It is believed, however, that for most cases the differences would be within acceptable engineering accuracy.

IV. Conclusion

Two popular duality-based approaches (i.e., "the reluctance based" and "the direct application") for derivation of low-frequency transformer models have been discussed, and their advantages and disadvantages have been highlighted. It was explained that the sources are easier to connect with the direct application of duality.

It has been shown that the models can be very different for transformers with different iron-core geometries and/or winding configurations. The optimum duality derived models change for different operating conditions as the pattern of the magnetic flux changes. Despite this fact, it has been shown that unified models can be introduced for a specific type of transformer to represent all low-frequency transients with acceptable accuracy. This is shown for single-phase shell-type transformers in this Part I of the paper.

The need for adding (series) inductors to represent the (parallel) flux for all magnetic core branches has been recognized when saturation of the core is expected.

The mathematical equivalency of three *leakage* models for three-winding transformers has also been discussed. It has been shown that the numerical instability that can occur when simulating three-winding transformers is due to an improper connection of the magnetizing branch; that is, numerical oscillations do not happen in topologically correct transformer models.

References

[1] E. C. Cherry, "The duality between interlinked electric and magnetic circuits and the formation of transformer equivalent circuits," in *Proc. Phys. Soc.*, Feb. 1949, vol. B, no. 62, pp. 101–111.

[2] G. R. Slemon, "Equivalent circuits for transformers and machines including nonlinear effects," in *Proc. Inst. Elect. Eng.*, 1953, vol. 100, no. 5, pp. 129–143, IV.

[3] G. R. Slemon, *Elect. Mach. Drives*. Reading, MA, USA: Addison-Wesley, 1992.

[4] H. Fraisse, J. P. Masson, F. Marthouret, and H. Morel, "Modeling of a non-linear conductive magnetic circuit part 2: Bond graph formulation," *IEEE Trans. Power Electron.*, vol. 31, no. 6, pp. 4068–4070, Nov. 1995.

[5] G. Gonzalez-A and D. Nuñez-P, "Electrical and magnetic modeling of a power transformer: A bond graph approach," *World Acad. Sci., Eng. Technol.*, vol. 6, no. 9, pp. 591–597, 2012.

[6] X. Chen, "A three-phase multi-legged transformer model in ATP using the directly-formed inverse inductance matrix," *IEEE Trans. Power Del.*, vol. 11, no. 3, pp. 1554–1562, Jul. 1996.

[7] W. G. Enright, "Transformer models for electromagnetic transient studies with particular reference to HVDC transmission," Ph.D. dissertation, Dept. Elect. Comput. Eng., Univ. Canterbury, Christchurch, New Zealand, 1996.

[8] R. W. Buntenbach, "Analogs between magnetic and electrical circuits," *Electron Prod.*, vol. 12, no. 5, pp. 108–113, Oct. 1969.

[9] D. C. Hamill, "Lumped equivalent circuits of magnetic components: The gyrator-capacitor approach," *IEEE Trans. Power Electron.*, vol. 8, no. 2, pp. 97–103, Apr. 1993.

[10] P. G. Blanken and J. J. L. M. van Vlerken, "Modeling of electromagnetic systems," *IEEE Trans. Magn.*, vol. 27, no. 6, pp. 4509–4515, Nov. 1991.

[11] P. G. Blanken, "A lumped winding model for use in transformer models for circuit simulation," *IEEE Trans. Power Electron.*, vol. 16, no. 3, pp. 445–460, May 2001.

[12] M. Lambert, J. Mahseredjian, M. Martinez-Duro, and F. Sirois, "Magnetic circuits within electric circuits: critical review of existing methods and new mutator implementations," *IEEE Trans. Power Del.*, vol. 30, no. 6, pp. 2427–2434, Dec. 2015.

[13] J. A. Martı´nez, R. Walling, B. Mork, J. Martin-Arnedo, and D. Durbak, "Parameter determination for modeling systems transients. Part III: Transformers," *IEEE Trans. Power Del.*, vol. 20, no. 3, pp. 2051–2062, Jul. 2005.

[14] J. A. Martı´nez and B. Mork, "Transformer modeling for low and mid-frequency transients—A review," *IEEE Trans. Power Del.*, vol. 20, no. 2, pt. 2, pp. 1625–1632, Apr. 2005.

[15] F. de León and A. Semlyen, "Complete transformer model for electromagnetic transients," *IEEE Trans. Power Del.*, vol. 9, no. 1, pp. 231–239, Jan. 1994.

[16] A. Narang and R. H. Brierley, "Topology based magnetic model for steady-state and transient studies for three phase core type transformers," *IEEE Trans. Power Syst.*, vol. 9, no. 3, pp. 1337–1349, Aug. 1994.

[17] C. M. Arturi, "Transient simulation and analysis of a three-phase five-limb step-up transformer following and out-of-phase synchronization," *IEEE Trans. Power Del.*, vol. 6, no. 1, pp. 196–207, Jan. 1991.

[18] X. Chen and S. S. Venkata, "A three-phase three-winding core-type transformer model for low-frequency transient studies," *IEEE Trans. Power Del.*, vol. 12, no. 2, pp. 775–782, Apr. 1997.

[19] B. A. Mork, "Five-legged wound-core transformer model: Derivation, parameters, implementation, and evaluation," *IEEE Trans. Power Del.*, vol. 14, no. 4, pp. 1519–1526, Oct. 1999.

[20] B. A. Mork, F. Gonzalez, D. Ishchenko, D. L. Stuehm, and J. Mitra, "Hybrid Transformer model for transient simulation: Part I: Development and parameters," *IEEE Trans. Power Del.*, vol. 22, no. 1, pp. 248–255, Jan. 2007.

[21] N. Chiesa, B. A. Mork, and H. K. Høidalen, "Transformer model for inrush current calculations: Simulations, measurements and sensitivity analysis," *IEEE Trans. Power Del.*, vol. 25, no. 4, pp. 2599–2608, Oct. 2010.

[22] A. Rezaei-Zare, "Enhanced transformer model for low-and mid-frequency transients—Part I: Model development," *IEEE Trans. Power Del.*, vol. 30, no. 1, pp. 307–315, Feb. 2015.

[23] S. E. Zirka, Y. I. Moroz, C. M. Arturi, N. Chiesa, and H. K. Høidalen, "Topology-correct reversible transformer model," *IEEE Trans. Power Del.*, vol. 27, no. 4, pp. 2037–2045, Oct. 2012.

[24] F. de León and J. A. Martinez, "Dual three-winding transformer equivalent circuit matching leakage measurements," *IEEE Trans. Power Del.*, vol. 24, no. 1, pp. 160–168, Jan. 2009.
[25] , J. A. Martinez-Velasco, Ed., *Power System Transients: Parameter Determination*. Boca Raton, FL, USA: CRC, 2010.
[26] C. Álvarez-Mariño, F. de León, and X. M. López-Fernández, "Equivalent circuit for the leakage inductance of multi-winding transformers: Unification of terminal and duality models," *IEEE Trans. Power Del.*, vol. 27, no. 1, pp. 353–361, Jan. 2012.
[27] S. Jazebi, F. de León, A. Farazamand, and D. Deswal, "Dual reversible transformer model for the calculation of low-frequency transients," *IEEE Trans. Power Del.*, vol. 28, no. 4, pp. 2509–2517, Oct. 2013.
[28] S. Jazebi and F. de León, "Experimentally validated reversible single-phase multi-winding transformer model for the accurate calculation of low-frequency transients," *IEEE Trans. Power Del.*, vol. 30, no. 1, pp. 193–201, Feb. 2015.
[29] S. Jazebi and F. de León, "Duality-based two-winding transformer model including eddy current effects in the windings," *IEEE Trans. Power Del.*, vol. 30, no. 5, pp. 2312–2320, Oct. 2015.
[30] E. P. Dick and W. Watson, "Transformer models for transient studies base on field measurements," *IEEE Trans Power App. Syst.*, vol. PAS-100, no. 1, pp. 409–419, Jan. 1981.
[31] V. Brandwajn, H. W. Dommel, and I. I. Dommel, "Matrix representation of three-phase N-winding transformers for steady-state and transient studies," *IEEE Trans Power App. Syst.*, vol. PAS-101, no. 6, pp. 1369–1378, Jun. 1982.
[32] M. Lambert, "Transformer modeling for low- and mid-frequency electromagnetic transients simulation," Ph.D. dissertation, École Polytechnique de Montréal, Montréal, QC, Canada, 2014.
[33] A. Boyajian, "Theory of three-circuit transformers," *Trans. Amer. Inst. Elect. Eng.*, vol. XLIII, pp. 508–529, Jan. 1924.
[34] L. F. Blume, A. Boyajian, G. Camilli, T. C. Lenox, S. Minneci, and V. M. Montsinger, *Transformer Engineering: A Treatise on the Theory, Operation, and Application of Transformers*. New York, USA: Wiley, 1951, p. 70.
[35] "Staff of the department of electrical engineering of massachusetts institute of technology," in *Magnetic Circuits and Transformers*. New York, USA: Wiley, 1943.
[36] X. Chen, "Negative inductance and numerical instability of the saturable transformer component in EMTP," *IEEE Trans. Power Del.*, vol. 15, no. 4, pp. 1199–1204, Oct. 2000.
[37] P. S. S. Holenarsipur, N. Mohan, V. D. Albertson, and J. Cristofersen, "Avoiding the use of negative inductances and resistances in modeling three-winding transformers for computer simulations," in *Proc. IEEE Power Eng. Soc. Winter Meeting*, 1999, pp. 1025–1030.
[38] T. Henriksen, "How to avoid unstable time domain responses caused by transformer models," *IEEE Trans. Power Del.*, vol. 17, no. 2, pp. 516–522, Apr. 2002.
[39] Slow Transients Task Force of the IEEE. Modeling and Analysis of System Transients Using Digital Programs Working Group, "Modeling and analysis guidelines for slow transients—Part III: The study of ferroresonance," *IEEE Trans. Power Del.*, vol. 15, no. 1, pp. 255–265, Jan. 2000.
[40] S. E. Zirka, Y. I. Moroz, and C. M. Arturi, "Accounting for the influence of the tank walls in the zero-sequence topological model of a three-phase, three-limb transformer," *IEEE Trans. Power Del.*, vol. 29, no. 5, pp. 2172–2179, Oct. 2014.
[41] M. Lambert, M. M. Duró, J. Mahseredjian, F. de León, and F. Sirois, "Transformer leakage flux models for electromagnetic transients: Critical review and validation of a new model," *IEEE Trans. Power Del.*, vol. 29, no. 5, pp. 2180–2188, Oct. 2014.
[42] F. de León, S. Jazebi, and A. Farazmand, "Accurate measurement of the air-core inductance of iron-core transformers with a non-ideal low-power rectifier," *IEEE Trans. Power Del.*, vol. 29, no. 1, pp. 294–296, Feb. 2014.

S. Jazebi (M'14), photograph and biography not available at the time of publication.

S. E. Zirka, photograph and biography not available at the time of publication.

M. Lambert (M'09), photograph and biography not available at the time of publication.

A. Rezaei-Zare (SM'10), photograph and biography not available at the time of publication.

N. Chiesa, photograph and biography not available at the time of publication.

Y. Moroz, photograph and biography not available at the time of publication.

X. Chen (SM'13), photograph and biography not available at the time of publication.

M. Martinez-Duro (M'09), photograph and biography not available at the time of publication.

C. M. Arturi (M'87), photograph and biography not available at the time of publication.

E. P. Dick (SM'14), photograph and biography not available at the time of publication.

A. Narang (SM'95), photograph and biography not available at the time of publication.

R. A. Walling (F'05), photograph and biography not available at the time of publication.

J. Mahseredjian (F'13), photograph and biography not available at the time of publication.

J. A. Martinez (SM'12), photograph and biography not available at the time of publication.

F. de León (F'15), photograph and biography not available at the time of publication.